THE INTERNATIONAL SOCIETY OF
PRECISION AGRICULTURE PRESENTS THE
13th INTERNATIONAL CONFERENCE ON
PRECISION AGRICULTURE
July 31-August 4, 2016 • St. Louis, Missouri USA

High resolution vegetation mapping with a novel compact hyperspectral camera system

P. Baeck[a], J. Blommaert[a], S. Delalieux[a], B. Delauré[a], S. Livens[a], D. Nuyts[a,], A. Sima[a], G. Jacquemin[b] and J.P. Goffart[b]

[a] VITO NV, Mol, Belgium,
[b] Centre Wallon de Recherches agronomiques (CRA-W), Gembloux, Belgium

A paper from the Proceedings of the
13th International Conference on Precision Agriculture
July 31 – August 4, 2016
St. Louis, Missouri, USA

Abstract.

The COSI-system is a novel compact hyperspectral imaging solution designed for small remotely piloted aircraft systems (RPAS). It is designed to supply accurate action and information maps related to the crop status and health for precision agricultural applications. The COSI-Cam makes use of a thin film hyperspectral filter technology which is deposited onto an image sensor chip resulting in a compact and lightweight instrument design.

This paper reports on the agricultural monitoring missions in 2015 which have been executed with the COSI-system over hundreds of experimental field plots containing 40 different varieties of winter wheat. In this experiment two different treatments have been executed one with fungicides and the other one without. In total 4 missions with a RPAS have been conducted over the test area. The paper describes the preliminary results of the discrimination between the different treatments as observed by the COSI-Cam.

Keywords. *hyperspectral, camera, infrared, vegetation health, RPAS.*

Introduction

Improving the spectral detail of earth observation from Remotely Piloted Aircraft Systems (RPAS) can greatly expand its potential for use in vegetation monitoring and specifically in precision agriculture. Due to the high spatial resolution the image product pixels can be very pure increasing the detection sensitivity to small anomalies in the field. This allows supplying detailed crop status information to the farmer of the crop in the form of an action and information containing the spatial variability over the complete field in terms of for instance plant health, vegetation stress or the presence of diseases and the evolution of them as a function of time when multiple missions are being executed. The advantage of hyperspectral in comparison to multispectral systems is that anomalies can be detected at an earlier stage to support a fast reaction and suitable counteracting measures.

Traditional hyperspectral pushbroom imagers observe a single line on the ground through a slit in the optical system dispersing the light and projecting it at a 2-dimensional detector. All spectral bands are simultaneously recorded for every ground location and a scanning motion is required to cover the area of interest. Although such devices are already available for RPAS and have already been flown on fixed- and rotary-wing platforms, the construction of geometrically correct image products requires high accuracy IMU and GNSS information which, usually comes along with the weight and cost of the device.

Interference filters with varying thickness are an alternative technology which allows constructing very compact hyperspectral imagers. When deposited as a wedge on a substrate and mounted close to a detector, this results in LVF (Linear Variable Filter) hyperspectral instruments. More recently, direct deposition of filters onto detectors has allowed creating different spatial configurations of the filters, including mosaic, tiled and stepwise line filters. Stepwise line filters typically have a small (e.g. 8) number of lines with the same spectral band. In an LVF based imager every pixel row in the image corresponds to a different spectral band as well as a different location on the ground. A scanning motion is required not only to cover the area of interest, but also to retrieve the complete spectrum for every point on the ground.

Such stepwise line filter is used in the COmpact hyperSpectral Imaging system (COSI) designed and developed by VITO. The system is designed to be operated on small remotely piloted aircraft systems (RPAS), with a payload capacity of less than 500g. This lightweight innovative camera system is sensitive to very subtle vegetation spectral differences and plant height differences. A photogrammetry based processing solution transforms the raw images as acquired by the camera into action and information maps indicating the status of the vegetation to support health, anomaly, disease and stress detection in an early phase. These action and information maps are expected to support decision making, and as such allow for more site and time specific field management.

COSI system

Hyperspectral camera

Conceptually the system is very similar to a standard digital camera as it acquires 2-dimensional images of the scene. However the hyperspectral capability, which allows to sense the visible and near infrared spectral range through narrow bands, is realized using a disruptive thin film filter technology which is directly deposited at the image sensor chip of the camera. The spectral bands are arranged per line, with groups of 5 to 8 adjacent lines having the same spectral response.

The imaging concept of the camera is shown in figure 1. The thin film filters were deposited on a 2 Megapixels high sensitivity CMOS image sensor by the micro-electronics laboratory Imec (Heverlee, Belgium), giving a continuous coverage of the 600 to 900 nm spectral range with 72 narrow band filter responses (FWHM 5 to 10 nm) . Presently a modified hyperspectral camera is in preparation covering a spectral range of 470 to 900 nm (Serruys et al., 2014).

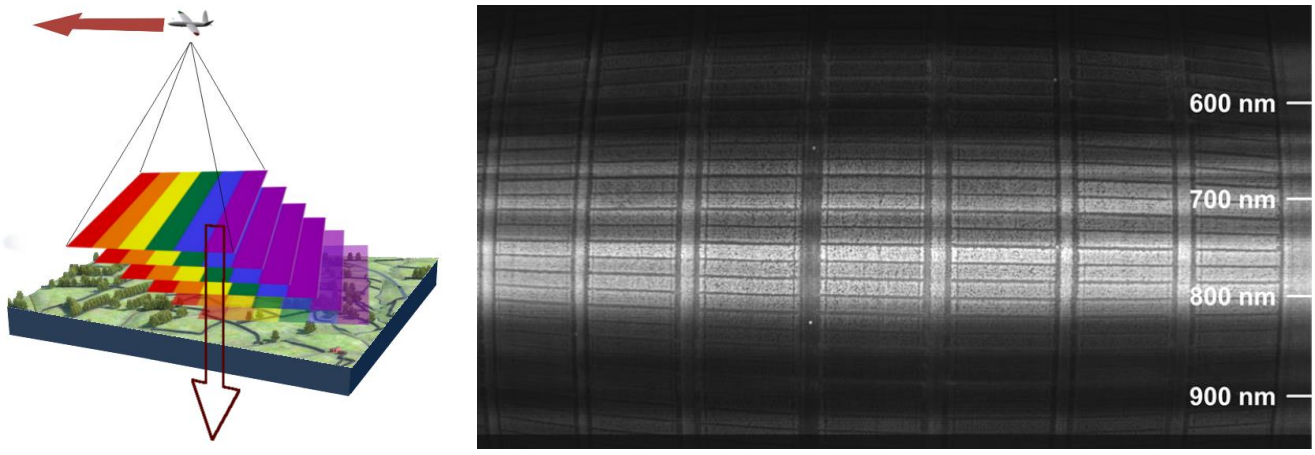

Figure 1. Imaging concept of the COSI-Cam with linear variable filter (left), a single raw image of the COSI-Cam (right)

A unique property of the specific camera design and processing approach is that it is able to produce maps with a very high spatial resolution (e.g. 3 cm from 60 m altitude). As a result the system allows to support single plant monitoring in for instance small experimental field plots of a few m² each and covering a total area of about 1 ha, as has been demonstrated using rotary wing RPAS. Embarked on a suitable fixed wing RPAS system the system is able to cover also larger areas of hundreds of ha in a single flight mission at resolutions of 10 cm which is more suitable for operational monitoring.

Image processing software

The image processing workflow is developed by VITO and involves several steps:

- pre-processing
- hyperspectral datacube generation
- raster calculation and compositing

During *pre-processing* the collected data are validated using quality checks on the flight and camera metadata and the raw images. Also, the images are enhanced and georeferenced using the on-board GPS. After that, the *hyperspectral datacube generation* is initiated. It includes aerial triangulation, bundle block adjustment, camera calibration and point cloud generation algorithms (Sima et al., 2016). Next, the hyperspectral bands are reconstructed from the individual images and radiometrically corrected (Livens et al., 2016). Lastly, the spectral indices and false-color composites are derived from *raster calculation and compositing* of the hyperspectral datacube.

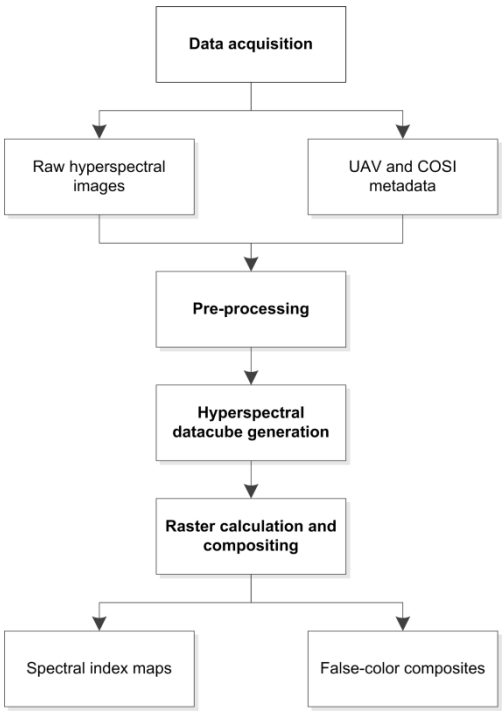

Figure 2. Flowchart of the image processing software workflow.

At VITO, an operational cloud processing environment has been set up, to allow users to upload their data on the local processing cluster with advanced processing nodes (12 CPU's, 64GB RAM, GPU support) for high speed processing. The entire workflow runs semi-automated: manual interactions are currently only needed for geometric and spectral ground control point identification and visual end-product validation.

Data products

The COSI image processing software supports four standard output data products:

- digital surface model
- hyperspectral datacube
- false-color image composite
- spectral index map

The **digital surface model** (DSM) represents the 3D model of the terrain's surface. The image processing software exports the digital surface model in the user defined coordinate system and format. For enhanced absolute spatial accuracy, ground control points can be introduced.

The **hyperspectral datacube** contains the surface reflection orthomosaic images of each single spectral band. The spectral range of the COSI-Cam as used in the winter wheat missions is 600 to 900 nm, while the spectral resolution is about 5 to 10 nm. For visual display, each band of the hyperspectral hypercube may be displayed one band at a time as a grey scale image, or in combination of three bands at a time as a color composite image. The **false-color image composite** provides a quick overview of the terrain vegetation. The false-color composition used is:

R = band 41 (800 nm; NIR)
G = band 15 (670 nm; red)
B = band 2 (605 nm; green)

In this type of false-color composite images, vegetation appears in different shades of red depending

on the types and conditions of the vegetation, since it has a high reflectance in the NIR band. Clear water appears dark-bluish (higher green band reflectance), while turbid water appears cyan (higher red reflectance due to sediments) compared to clear water. Bare soils, roads and buildings may appear in various shades of blue, yellow or grey, depending on their composition (Liew, 2001).

The **spectral index map** is a graphical indicator for specific terrain analysis. Different bands may be combined to accentuate e.g. the vegetated areas. One of the oldest combinations is the *Normalized Difference Vegetation Index (NDVI)* . The combination of its normalized difference formulation and use of the highest absorption and reflectance regions of chlorophyll make it robust over a wide range of conditions. It can, however, saturate in dense vegetation conditions when Leaf Area Index LAI becomes high. NDVI is computed by band 15 (670 nm) and band 41 (800 nm):

$$NDVI = (band\ 41 - band\ 15) / (band\ 41 + band\ 15) \quad (1)$$

The value of this index ranges from -1 to 1. The common range for green vegetation is 0.2 to 0.8 (Roose et al., 1973).

Another used vegetation index is the *Red Edge Normalized Difference Vegetation Index (ReNDVI)*, which is a modification of the traditional broadband NDVI and differs by using bands along the red edge, instead of the main absorption and reflectance peaks. Applications include precision agriculture, forest monitoring, and vegetation stress detection. The ReNDVI capitalizes on the sensitivity of the vegetation red edge to small changes in canopy foliage content, gap fraction, and senescence. ReNDVI is computed by band 22 (705 nm) and band 31 (750 nm):

$$ReNDVI = (band\ 31 - band\ 22) / (band\ 31 + band\ 22) \quad (2)$$

The value of this index ranges from -1 to 1. The common range for green vegetation is 0.2 to 0.9 (Gitelson et al., 1994 and Sims et al., 2002). Besides these two examples, many more relevant spectral indices can be generated from the hyperspectral datacube, highlighting different biophysical aspects of the soil, crop growth and crop condition.

Study area

The study area is located in Gembloux-Liroux, Belgium and focuses on growth of winter wheat. Figure 3 and 5 show the location of the study area. The winter wheat experiment consists of 40 cultivars. They were randomized over 8 rows of 40 plots each with a size of 1.5 x 10-m and a 250-grains/m² seeding density. Half of the rows were treated with fungicides for a total of 3.85 L/ha (row A1, A2, A3 and A4 in figure 5).

Figure 3. Winter wheat field plots (1.5 x 10 m) at Gembloux-Liroux, Belgium (7 July 2015)

Figure 4. COSI camera mounted on the Aerialtronics Zenith octocopter

At different moments in time visual inspections have been executed to assess the degree of infection of the field plot to the following three diseases: yellow rust, brown rust, septoriosis. A shape file has been defined for each individual plot to execute the data analysis on each plot. The delineation of the

plots was somewhat smaller to eliminate possible boundary effects. The effective area which has been taken into account for the analysis is 64 x 96 m².

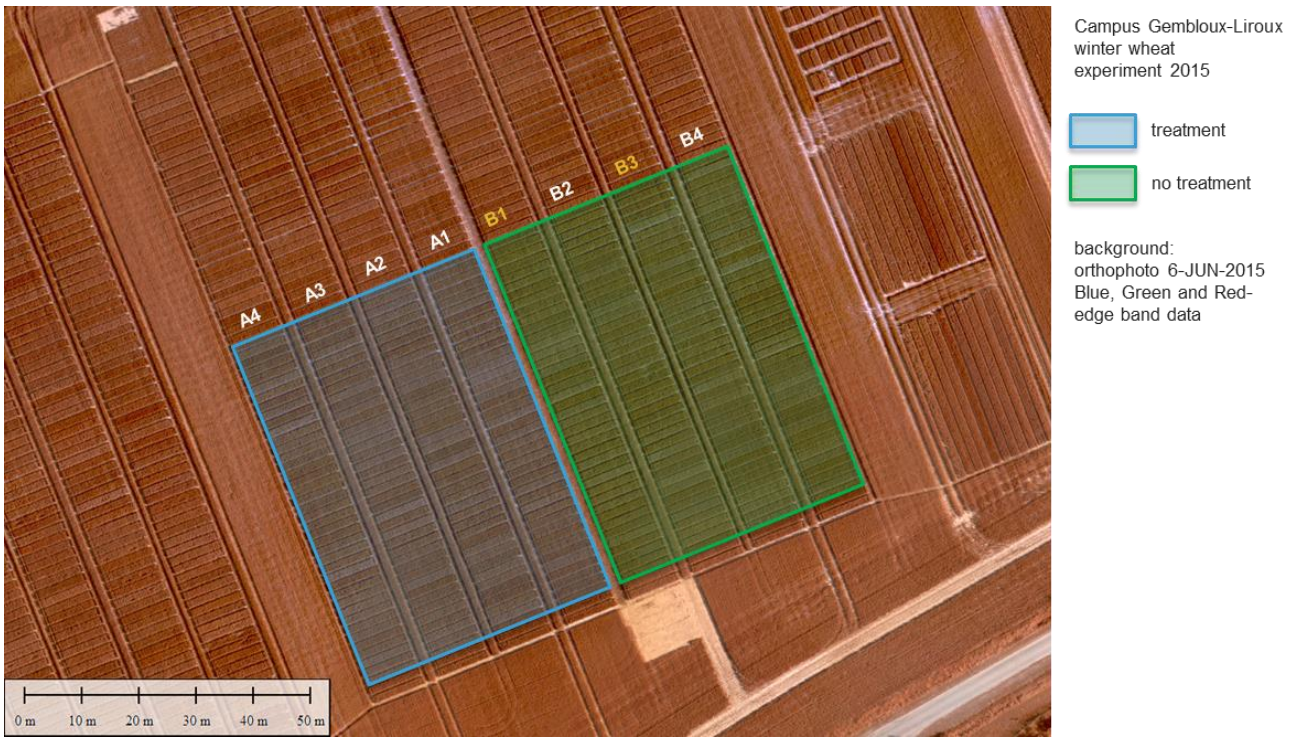

Figure 5. Study area: winter wheat experiment at Gembloux-Liroux (Belgium) agricultural research station in 2015

Regular visual ground observations for disease occurrence (yellow rust, brown rust and septoriosis) took place on 2 rows with no fungicides treatment (row B1 and B3 in figure 2). In total, 4 UAV flights with the COSI camera were executed (table 1). The UAV dataset at June, 12th 2015 is cropped on the left side of the field, due to the extreme variations in light conditions during a part of the flight campaign.

Table 1: Details of COSI flight campaigns and disease observations

Type	Date	Number of images	Weather conditions
Yellow rust + septoriosis	3 May 2015		
UAV	11 May 2015	10.581	good
UAV	22 May 2015	10.591	good
Yellow rust + septoriosis	25 May 2015		
Yellow rust + septoriosis + brown rust	5 June 2015		
UAV	12 June 2015	9.810	varying light conditions
Yellow rust + brown rust	14 June 2015		
Yellow rust + septoriosis + brown rust	24 June 2015		
UAV	7 July 2015	10.022	good

In this study we used the octocopter Aerialtronics Altura AT8 and Altura Zenith (see figure 4). Based on image processing requirements such as spectral band overlap, image side overlap, ground sample distance (GSD) and the region of interest (ROI) the flight, platform and camera parameters are chosen (see table 2). Flying at 80 m above ground level results in a GSD of 4.0 cm. The COSI camera captures images at a continuous rate of 28 fps and with exposure time set according to the light conditions.

Table 2: COSI flight campaign parameters

GSD	4.0 cm
Spectral band overlap	60 %
Image side overlap	80 %
ROI	64 x 96 m
COSI frame rate	28 fps
Platform speed	3.6 m/s
Flight height	80 m
Flight lines	8
Flight time	10 minutes

Image products

The digital surface models were generated without using ground control and were exported in TIF-image format. The DSM represents the crop surface and can be abstracted from a ground model in order to obtain the plant height (Bending et al., 2014). The DSM was visualized in ENVI 4.7 and clipped with the region of interest. Figure 6 clearly shows the individual cultivars and the slope of the entire study area.

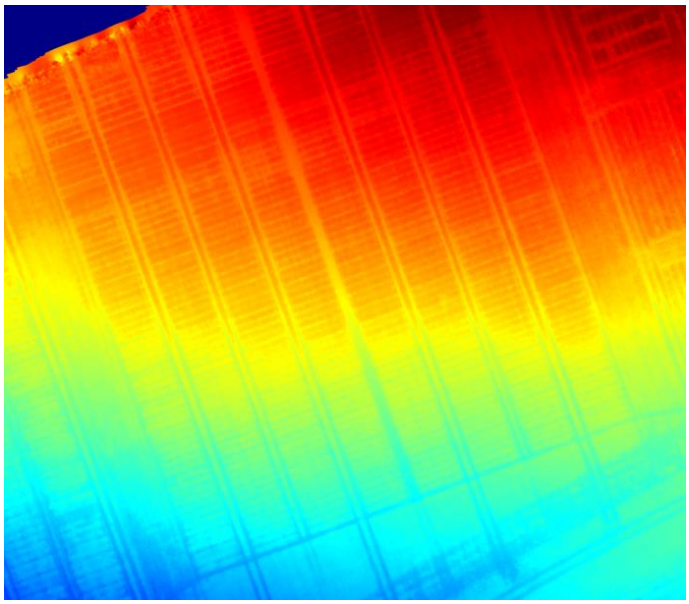

Figure 6. Digital Surface Model (Gembloux, 22-May-2015)

For each spectral band, the image processing software writes out the surface reflection orthomosaic in ENVI format. Three single spectral bands and the false color composite were visualized in ENVI 4.7 as grey scale images. Figure 7 shows band 1 (600 nm), band 25 (720 nm) and band 41 (800 nm) of the dataset at July, 7th 2015. Figure 8 displays the false color composite and figure 9 contains the NDVI maps for the four different flight campaigns.

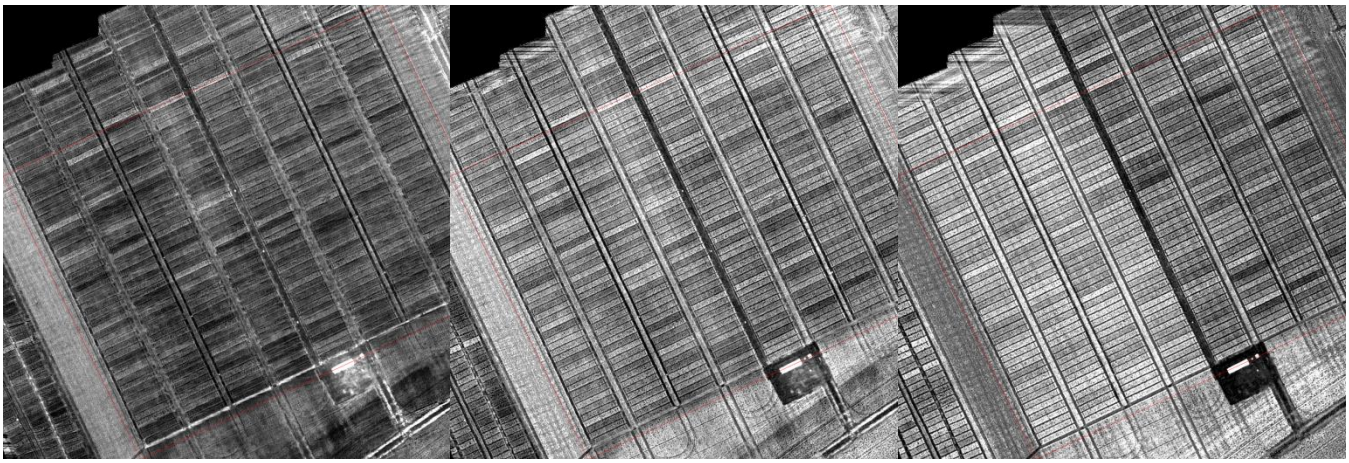

Band 1 (600 nm) **Band 25 (720 nm)** **Band 41 (800 nm)**

Figure 7. Surface reflection at 3 different wavelengths (Gembloux, 7-July-2015)

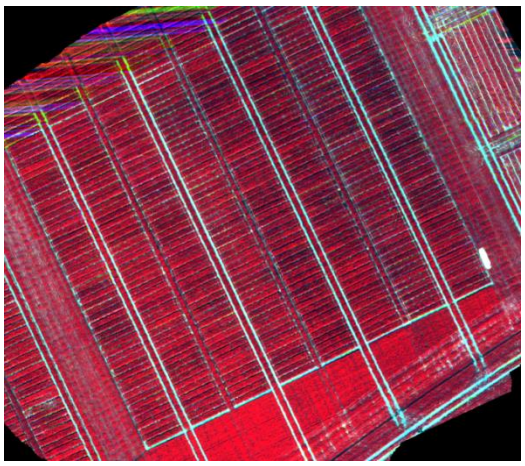

11-May-2015

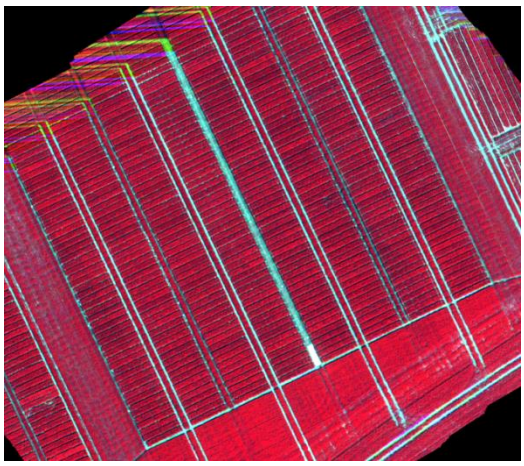

22-May-2015

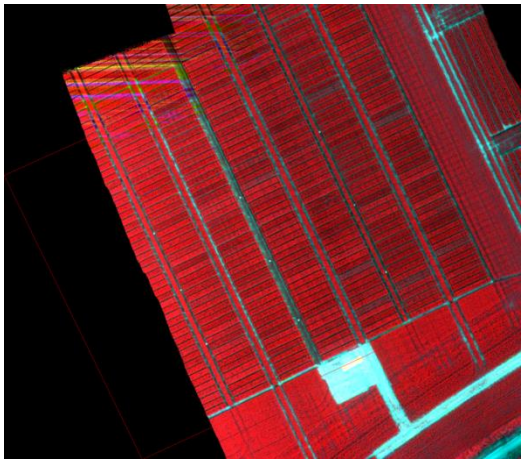

12-June-2015

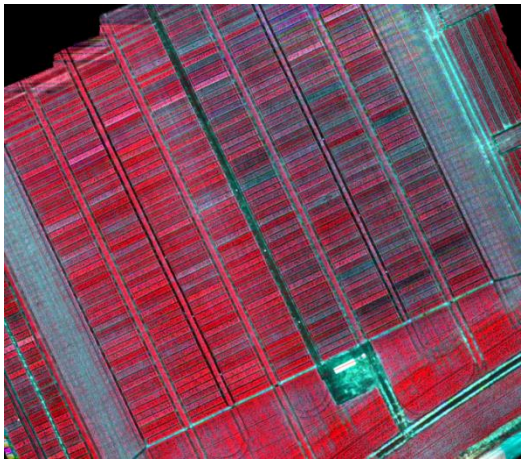

7-July-2015

Figure 8. False-color composites (Gembloux)

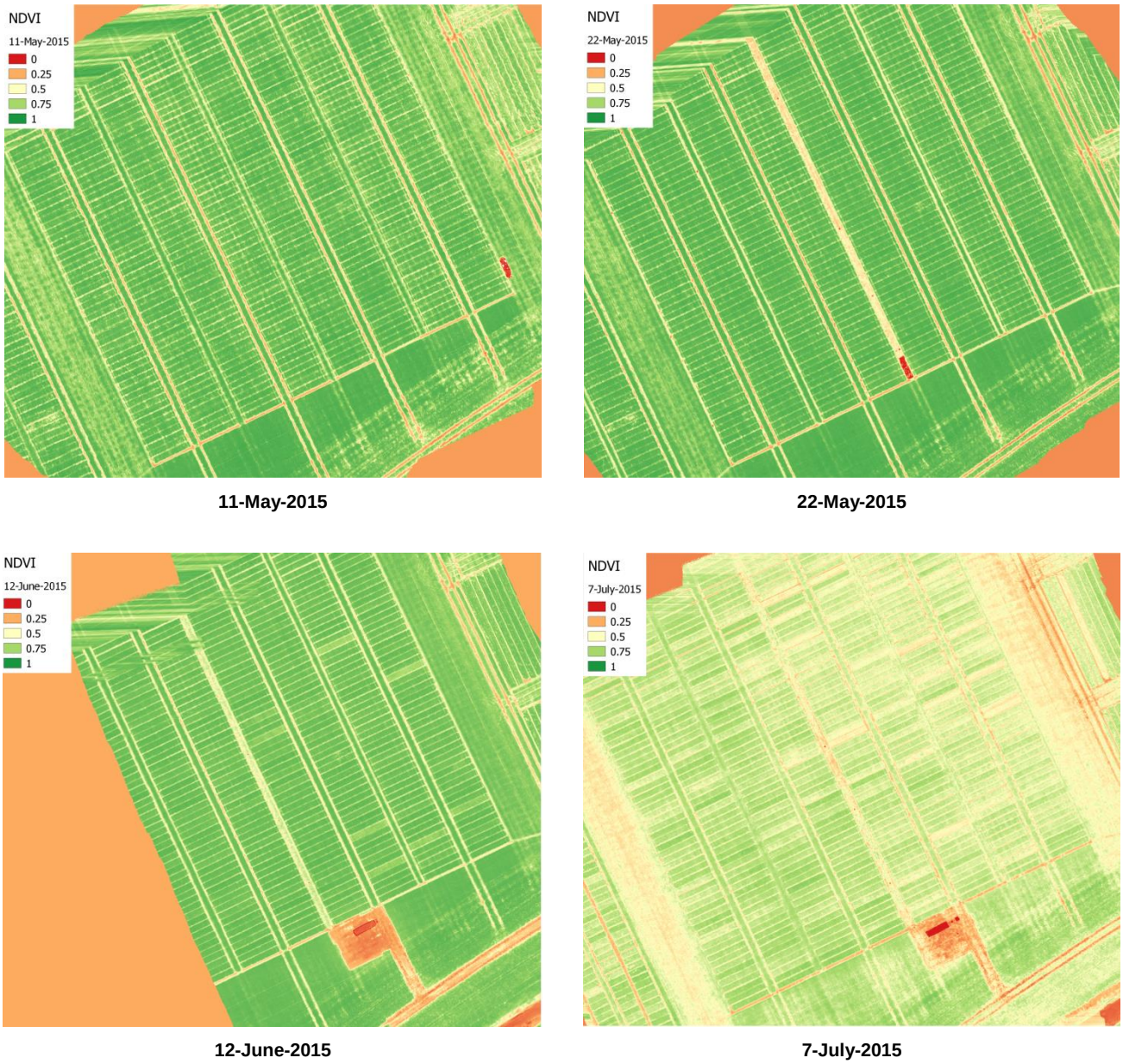

Figure 9. NDVI (Gembloux)

Analysis

Data analysis has been performed on a selection of 12 out of the 40 based on the following rationale. For each disease (yellow rust, brown rust and septoriosis) which has been evaluated based on the field inspection, the three varieties with the strongest infection are selected. From the 40 varieties also the 3 varieties with the lowest overall score in terms of degree of infection to all diseases were inspected.

For clarity, the spectrum of only one variety per group with and without fungicides treatment has been shown in figure 10. In the NIR range, an obvious and strong increase of reflectance over time can be observed. The reflectance values are pronounced higher for plots in the treated zone, especially at later stages of the growing season. Also, the reflectance slope in the NIR area

increases between 800 – 850 nm for plots in the untreated zone, while the treated plots show a more equal reflectance in this region.

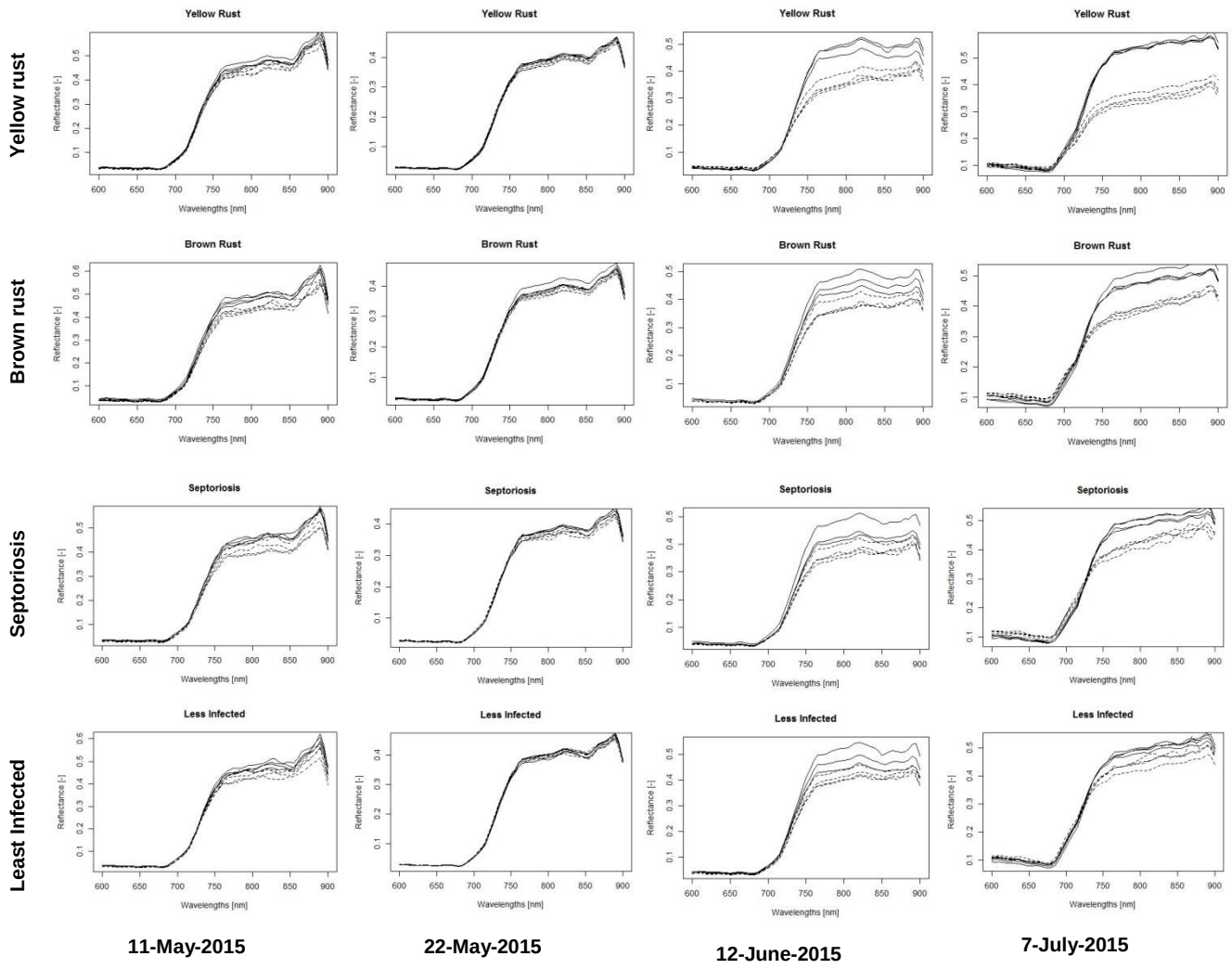

Figure 10. Average reflectance spectra for the 12 selected plots for the different RPAS missions. The dashed lines are plots without fungicides treatment, the solid lines are plots with fungicides treatment.

An example of a vegetation index calculation for the different groups is shown in figure 11. The **Modified Soil Adjusted Vegetation Index (MSAVI)** attempts to minimize brightness-related soil effects by considering first order soil vegetation interaction. It is defined by band and band 15 (670 nm) and band 41 (800 nm):

$$\mathrm{MSAVI} = \frac{2 * (\mathrm{band}\ 41) + 1 - \sqrt{2 * (\mathrm{band}\ 41 + 1)^2 - 8(\mathrm{band}\ 41 - \mathrm{band}\ 15)}}{2}$$

The value of this index ranges from -1 to 1 and represents vegetation greenness (Qi et al., 1994). During crop growth, an increase of the index is expected, while at the end of the growth season the index decreases. In case of disease, the efficiency of the photosynthesis and chlorophyll content diminishes, resulting in a lower MSAVI value. During the growing season differences between treated and non-treated zones become more pronounced, especially for yellow rust.

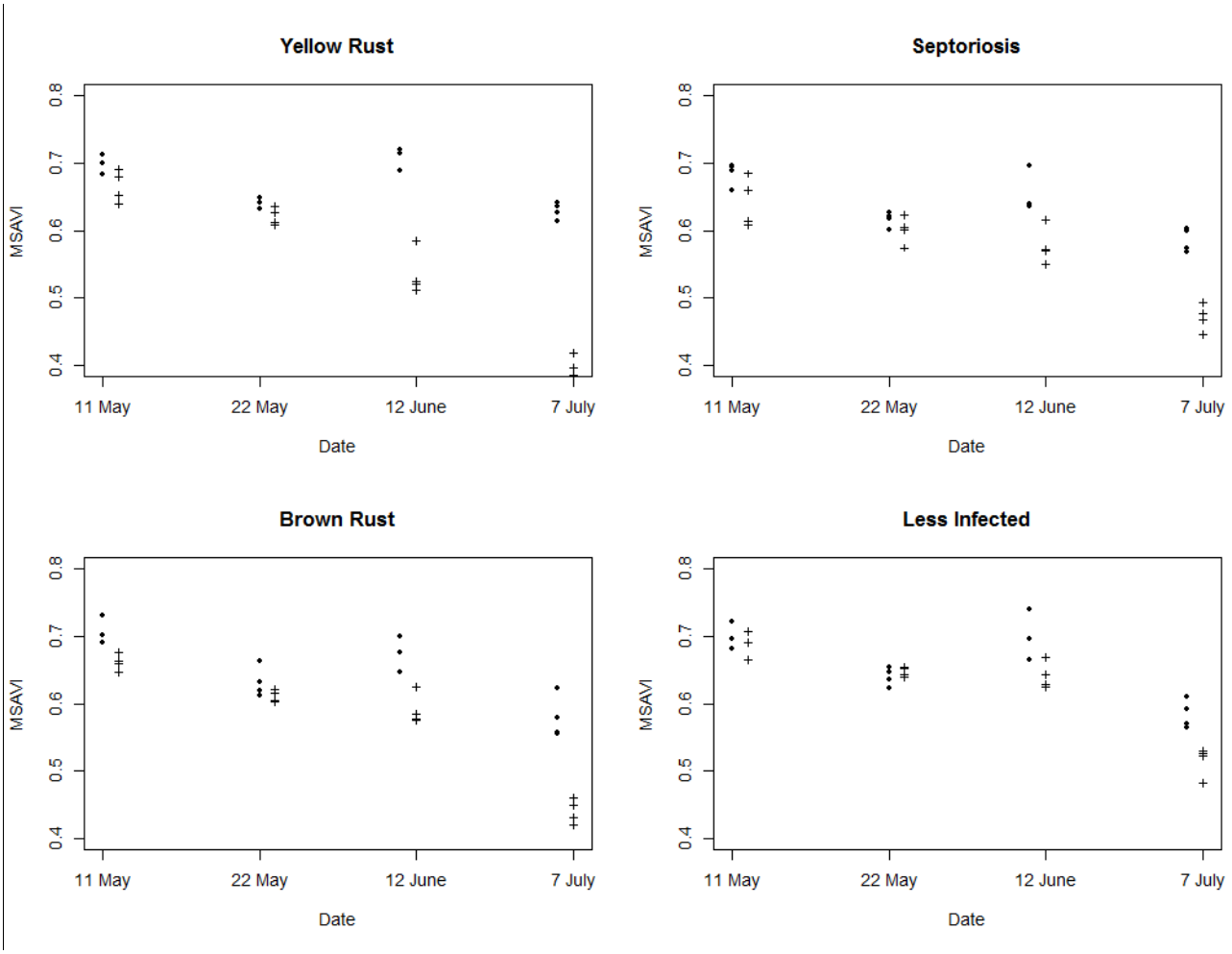

Figure 11. MSAVI: Modified Soil Adjusted Vegetation Index. Dots are plots without fungicides treatment, crosses are plots with fungicides treatment.

Conclusion

The camera is able to derive reflectance spectra which are sufficiently accurate to be used to reliably estimate important characteristics of agricultural fields at plot level. The spectra in the 600 – 900 nm range allow deriving a large number of different parameters. This includes the most commonly used vegetation indices, which are typically calculated from a small number of spectral bands. Importantly, having full spectra also allows deriving more advanced parameters, such as the REIP.

The spectra were studied at plot level. Scaling to higher resolutions, up to pixel level, is still under study. It must be noted that a fundamental limitation is posed by physical reflectance variations in the plots, which are mostly larger than measurement variations caused by the instrument.

Acknowledgements

We would like to thank IMEC for their support on the calibration of the camera system, Gert Strackx for his outstanding support in camera development, as well as the UAV pilot Tom Verstappen for his engagement in safe and successful data acquisition. Part of the COSI camera development was funded by the EC FP7 Airbeam security project.

References

Bendig, J., Bolten, A., Bennertz, S., Broscheit, J., Eichfuss, S., and Bareth, G. (2014): Estimating biomass of barley using Crop Surface Models (CSMs) derived from UAV-Based RGB Imaging. Remote Sensing, 6 (11), pp. 10395-10412. doi:10.3390/rs61110395.

Gitelson, A., Merzlyak, M. (1994). Spectral Reflectance Changes Associated with Autumn Senescence of Aesculus Hippocastanum L. and Acer Platanoides L. Leaves. Journal of Plant Physiology 143: 286-292.

Qi, J., Chehbouni, A., Huete, A.R., Kerr, Y.H. (1994). Modified Soil Adjusted Vegetation Index (MSAVI). Remote Sens Environ 48:119-126.

Liew, S. (2001). Interpretation of Optical Images, Centre for Remote Imaging, Sensing and Processing, Tutorial document. http://www.crisp.nus.edu.sg/~research/tutorial/opt_int.htm. Accessed 10 May 2015.

Livens, S., Blommaert, J., Nuyts, D., Sima, A., Baeck, P.-J., Delauré, B. (2016). Radiometric calibration of the COSI hyperspectral RPAS camera, in: Proceedings of 8th Workshop of Hyperspectral Image and Signal Processing: Evolution in Remote Sensing, Los Angeles 21-24 August 2016. In press.

Rouse, J., Haas, R., Schell, J., and Deering, D. (1973). Monitoring Vegetation Systems in the Great Plains with ERTS. Third ERTS Symposium, NASA : 309-317.

Serruys, P., Sima, A., Livens, S., Delauré, B., (2014). Linear Variable Filters – a Camera System Requirement Analysis for Hyperspectral Imaging Sensors Onboard Small Remotely Piloted Aircraft Systems, in: 6th Workshop on Hyperspectral Image and Signal Processing: Evolution in Remote Sensing, 24-27 June 2014, Lausanne, Switzerland. Lausanne, Switzerland, pp. 1–4.

Sima, A., Baeck, P., Nuyts, D., Delalieux, S., Livens, S., Blommaert, J., Delauré, B., Boonen, M. (2016). Compact hyperspectral imaging system (COSI) for small remotely piloted aircraft systems (RPAS) – system overview and first performance evaluation results. ISPRS Congres, Prague. In press.

Sims, D., Gamon, J. (2002). Relationships Between Leaf Pigment Content and Spectral Reflectance Across a Wide Range of Species, Leaf Structures and Developmental Stages. Remote Sensing of Environment 81: 337-354.